

# A Neuromorphic VLSI Implementation of a Simplified Electrosensory System in a Weakly Electric Fish

S. A. Aamir<sup>1</sup>, J. Engelmann<sup>1</sup>, L. Gomez<sup>2</sup>, and E. Chicca<sup>1</sup>

<sup>1</sup> Cognitive Interaction Technology - Center of Excellence (CITEC), University of Bielefeld, Universitätsstrasse 21-23, Bielefeld, Germany

<sup>2</sup> Facultad de Ciencias, Universidad de la Republica, Laboratorio de Neurociencias, Uruguay

Found in African rivers, the weakly electric Mormyrid fish *Gnathonemus petersii* generates an electric field around itself that it uses for active electrolocation, object detection and navigation [1]. We present a modeling study of sensory system of this weakly electric fish based on spiking neurons and compatible with an analog neuromorphic VLSI implementation. Our results demonstrate that the simulated neural network faithfully reproduces key features of the biological system. The neuromorphic emulation, currently being implemented on a multi-chip Address Event Representation (AER) based system [2, 3], will provide a powerful tool for exploring hypotheses derived by neurophysiological experiments. Further, it will help in evaluation of novel computational approaches for efficient, real-time computation of data produced by near-range sensing devices.

The Mormyrid fish generates a weak electric field by short synchronous activation of modified muscles cells in its tail (Electric Organ Discharge (EOD)). Distortions in the field are sensed by electroreceptors on the skin and the 2D distribution of the local field properties provide a basis to decode environmental parameters. In the absence of field distortion, i.e., in absence of a nearby target, the 2D distribution is homogeneous and the electroreceptor afferents respond with stereotyped burst of 1-4 spikes per EOD. Any perturbation of the field due to nearby objects, affects the spiking pattern, resulting in a change of both the number of spikes per EOD and their latency in proximate skin regions. The profile of the electric image, i.e. the 2D pattern of the perturbed field depends on the size and distance of the object [4]. The afferent spiking pattern encodes this electric image, such that higher Local Electric Organ Discharge (LEOD) intensities evoke early spikes (shorter latencies) and vice versa. The peripheral 2D activity pattern gets mapped through the primary afferents (Afs) into the Electrosensory Lateral Line Lobe (ELL) [5]. The sensory afferent input gets conveyed through the granulars (Grs) which receive and integrate multiple convergent afferent inputs. These granular cells provide inhibitory input to local interneurons (medium ganglions (Mgs)) and excitatory input to one class of output neurons (large fusiforms (Lfs)) of the ELL [6]. The GABAergic interneurons in turn make inhibitory connections to the output neurons [7]. All cells within the ELL also receive gating and modulating feedback from higher brain areas (Electric Organ Corollary Discharge (EOCD)).

In this work, we focus on a simplified one dimensional model of the ELL. The ELL network (whose basic connectivity is shown in Fig. 1a) is simulated in Brian [8] in order to test the feasibility of a hardware implementation. Our software model simulates the dynamics of the neuromorphic neurons, therefore providing an accurate predictor of the analog VLSI implementation.

In accordance with a simplified connectivity of the ELL, the patch of the modeled network contains 100 Afs, 200 Grs, 100 Mgs and 100 Lfs. A key element in this network is the inhibitory coupling between Mgs and Lfs upon excitation through the afferents. This leads to a delayed *disinhibition*, making Lf output neurons respond with a fixed number of spikes (in response to the LEOD), irrespective of the basal EOD amplitude (DC) and hence comparable to the biological system. Our simulation results (Fig. 1b) further replicate the latency pattern of Af cells which depends on the LEOD intensity, and is reflected in the response of the Lfs. The temporal jitter observed in the raster plots of Fig. 1b is caused by a random spread of one standard deviation ( $\sigma$ ), added to the leakage current parameter of the neuron model. This was introduced to mimic the variation in response properties of implemented neuromorphic neurons, occurring as a result of inherent device-mismatch effects <sup>1</sup> in analog circuits and transistors operated in weak inversion regime [10].

The model is robust to deviations in the spike-times as shown by the constancy of the Lf discharge pattern. To systematically evaluate the network performance, we run the simulation for different DC and LEOD values. The network response is characterized in terms of the inverse of first spike latency for the Lf population, as shown in Fig. 1c. As expected, there is a positive correlation between inverse latency and LEOD amplitude. Null values indicate the absence of Lf response.

<sup>1</sup> “time-independent random variations in physical quantities of identically designed devices” [9]

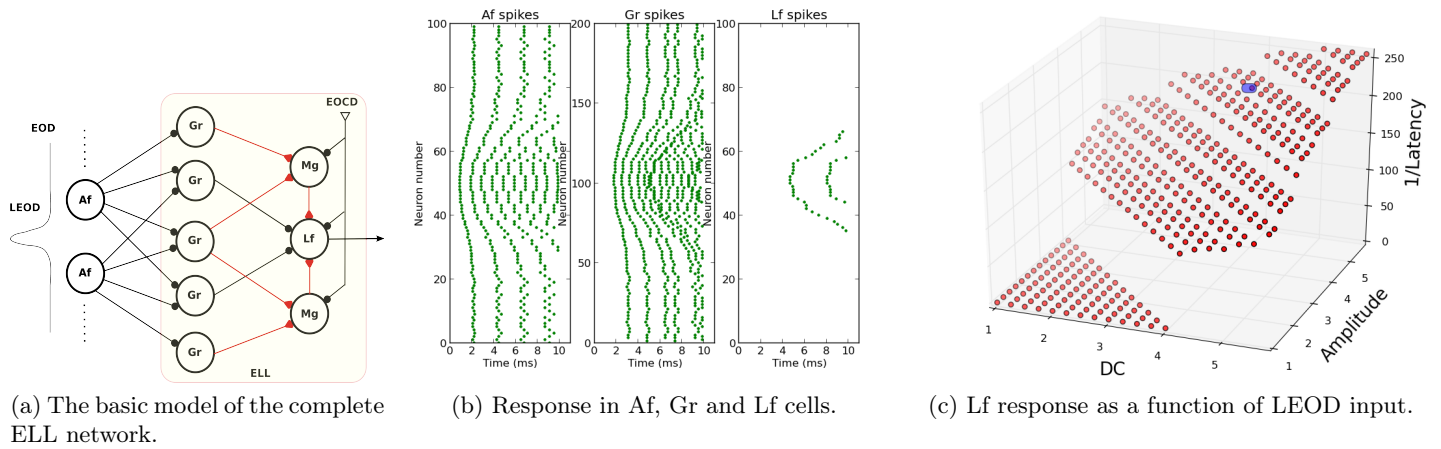


Fig. 1: (a) The basic model of the complete ELL network. The schematic diagram depicts how various neurons influence the spiking activity of a single Lf as projection neuron. In every EOD cycle, the LEOD evokes spikes in the Af population. The Gr layer comprises both excitatory as well as inhibitory neurons (which affect Lf via Mgs), while the EOCD shapes the Lf response by gating the input spikes both directly and via the inhibitory Mgs. (b) Raster plot of the Af, Gr, Lf spiking pattern, during an EOD cycle with a strong stimulus (LEOD profile). The spiking pattern in all three layers is shaped by stimulus intensity. Early spikes are recorded for higher intensity stimulus (hence shorter latencies). This latency encoding is visible in all layers and make the Lfs spike in a central region only. The Mg inhibition prevents the Lfs to spike at DC, as visible by absence of spikes in neurons numbered 0–35 and 65–100. The visible jitter in spike times among adjacent individual neurons is due to the implemented mismatch among individual neurons. (c) Inverse latencies plotted as a function of LEOD intensity parameters i.e., its amplitude and DC offsets. At lower DC values Lfs fail to elicit spikes, until a certain level is attained where input DC and amplitude is considerably high enough for Lf to spike (besides the inhibition from Mgs). Increasing inverse latencies depict an earlier firing in time, due to higher LEOD intensities as visible at the top right corner of the 3D plot. The Lf spiking response shown in (b) is highlighted on the 3D plot (c) with the blue shade.

The simplified circuit model of the Mormyrid fish ELL obtained here, present us with an initial insight into the role of different neuronal populations. This architecture reproduces biological observations and can be used to investigate the importance of other neurons observed in the biological system but not yet included in the modeling work. Given the temporal nature of the code, a computationally intensive spiking neural network is required, as opposed to mean frequency models, in order to capture the biological template. For this a fully parallel analog VLSI implementation offers a unique platform to test hypotheses about temporal coding and the influence of real electrosensory flow properties on the network.

## References

- [1] G. von der Emde and J. Engelmann, *Encyclopedia of Fish Physiology: From Genome to Environment*, vol. 1, Elsevier Inc., 2011.
- [2] D. B. Fasnacht, A. M. Whatley, and G. Indiveri, "A serial communication infrastructure for multi-chip address event system," in *International Symposium on Circuits and Systems, ISCAS 2008*. IEEE, May 2008, pp. 648–651.
- [3] D. B. Fasnacht and G. Indiveri, "A PCI based high-fanout AER mapper with 2 GiB RAM look-up table, 0.8  $\mu$ s latency and 66 mhz output event-rate," in *Conference on Information Sciences and Systems, CISS 2011*, Johns Hopkins University, March 2011, pp. 1–6.
- [4] R. Budelli and A. A. Caputi, "The electric image in weakly electric fish: perception of objects of complex impedance," *The Journal of Experimental Biology*, vol. 203, no. 3, pp. 481–92, Feb. 2000.
- [5] L. Gómez, R. Budelli, K. Grant, and A. A. Caputi, "Pre-receptor profile of sensory images and primary afferent neuronal representation in the mormyrid electrosensory system.," *The Journal of Experimental Biology*, vol. 207, no. 14, pp. 2443–53, Jun. 2004.
- [6] J. Meek, K. Grant, and C. C. Bell, "Structural organization of the mormyrid electrosensory lateral line lobe," *The Journal of Experimental Biology*, vol. 202, pp. 1291–1300, May 1999.
- [7] C. C. Bell, J. Meek, and J. Y. Yang, "Immunocytochemical identification of cell types in the mormyrid electrosensory lobe," *The Journal of Comparative Neurology*, vol. 483, no. 1, pp. 124–42, Feb. 2005.
- [8] D. Goodman and R. Brette, "The Brian simulator," *Frontiers in Neuroscience*, vol. 3, no. 2, pp. 192–197, 2009.
- [9] M. J. M. Pelgrom, A. C. J. Duinmaijer, and A. P. G. Welbers, "Matching properties of MOS transistors," *IEEE Journal of Solid-State Circuits*, vol. 24, no. 5, pp. 1433–1440, Oct. 1989.
- [10] S.-C. Liu, J. Kramer, G. Indiveri, T. Delbruck, and R. J. Douglas, *Analog VLSI: Circuits and Principles*, MIT Press, 2002.